Cytotoxic activity of pentachlorophenol and its active metabolites in SH-SY5Y neuroblastoma cells

Desiree Linda Fraser,[1] Barend Andre Stander,[1] Vanessa Steenkamp[2]

[1] Department of Physiology, Faculty of Health Sciences, University of Pretoria, Pretoria, South Africa

[2] Department of Pharmacology, Faculty of Health Sciences, University of Pretoria, Pretoria, South Africa

Corresponding author: Prof V Steenkamp

Postal address: Department of Pharmacology, Faculty of Health Sciences, School of Medicine, University of Pretoria, Private Bag X323, Arcadia, 0007, Pretoria, South Africa

Tel: +27 12 319 2547

E-mail address: vanessa.steenkamp@up.ac.za

Highlights

- The parent compound and metabolites each expressed different mechanisms of toxicity
- G1, S, and G2/M cell cycle blocks occurred due to PCP, TCBQ, and TCHQ exposure, respectively
- Mode of cell death was initially apoptosis which was converted to necrosis for TCHQ and PCP, but classic apoptosis for TCBQ
- Redox damage was secondary to MMP disruption for all compounds, and transient MMP recovery was found following TCHQ exposure
- TCHQ induced acetylcholinesterase inhibition, but not TCBQ or PCP

Abstract

As knowledge regarding mechanisms of pentachlorophenol (PCP) toxicity in neuronal cell lines is limited, the aim of the study was to evaluate the effects of PCP and its active metabolites, tetrachloro-1,4-benzoquinone (TCBQ) and tetrachlorohydroquinone (TCHQ) in human neuroblastoma SH-SY5Y cells. All compounds induced cytotoxic effects in time-dependent and dose-dependent manners, and resulted in differential modes of cell death. Reduced mitochondrial membrane potential (ΔΨM) and oxidative damage lead to apoptosis and necrosis following TCBQ and PCP exposure, respectively. Time-dependent investigations revealed transient ΔΨM recovery in TCHQ exposed cells, and redox stress. Sufficient ΔΨM recovery allowed apoptosis completion in TCHQ exposed cells, whereas overwhelming metabolic and oxidative stress saw a conversion from apoptotic to necrotic-like cell death. The onset of mitochondrial dysfunction preceded that of redox damage for all compounds, indicating that oxidative damage is secondary to ΔΨM insult. Cytotoxic events were further linked to cell cycle. S phase and G2/M blocks were observed after 12 h exposure to TCBQ and TCHQ, respectively, while a G1 block occurred after 24 h exposure to PCP. This study provides new insight regarding time-dependant toxic effects of PCP and its metabolites in human neuronal cells.

Key words: cell death; mitochondrial membrane potential; oxidative stress; pentachlorophenol; tetrachloro-1,4-benzoquinone; tetrachlorohydroquinone

1. Introduction

Pentachlorophenol (PCP) is an organochloride pesticide that is ubiquitous within the environment due to its chemical stability (Jones and de Voogt 1999). It is classified as a persistent organic pollutant, and has been predominantly used in the wood preservation industry. Concern and awareness regarding the toxicity of PCP has grown in recent years. Workers and populations living close to areas where PCP is frequently used and produced are at risk of chronic exposure, which may cause damage to human bodily functioning due to the bioaccumulation of PCP (Proudfoot 2003).

Pentachlorophenol has been linked to multiple types of cancer, and has been shown to be clastogenic in mammalian cells *in vitro*, as well as in lymphocytes of exposed persons *in vivo* (Ateeq et al. 2002). Adverse effects of PCP have been reported to varying degrees in the immune, hepatic, and endocrine systems (Guo and Zhou 2013; Schroeder 2011). Pentachlorophenol is lipophilic and is able to accumulate within the brain (Geyer et al. 1987), making neuronal cells at risk and susceptible to toxicity. Neurological effects have been reported for PCP exposure (ATSDR 2001). Characterisation of the mechanisms of toxicity in neuronal cells is essential for understanding and addressing the multiple facets of PCP effects in humans, as adverse effects of exposure may arise due to damage to neuronal tissue or cells. PCP is partially metabolised into two main active metabolites of interest: tetrachloro-1,4-benzoquinone (TCBQ), and tetrachlorohydroquinone (TCHQ) (Juhl et al. 1985). Pentachlorophenol has the ability to uncouple oxidative phosphorylation in the mitochondria, leading to excessive heat production and accentuated metabolism (Proudfoot 2003).

Uncoupling of oxidative phosphorylation in PCP exposed cells may lead to disrupted mitochondrial functioning, redox imbalances, caspase activation, cell cycle disruption, and ultimately death of exposed neuronal cells (Chen et al. 2015; Folch et al. 2009; Fu et al. 2016). Oxidative stress and DNA damage has been reported to play a role in its toxicity in different cell lines, particularly with regard to the metabolites (Li et al. 2017; Xu et al. 2018; Zhao et al. 2014), however responses appear to differ between cell lines. TCHQ seems to be a more toxic form of the xenobiotic that is able to induce DNA strand breakage, protein adducts, and depletion of glutathione content in liver tissue (Wang et al. 1997; Wang and Lin 1995).

Long-term exposure has also been reported to result in chronic fatigue or neuropsychiatric features in combination with skin infections (including chloracne), chronic respiratory symptoms, neuralgic pains in the legs, and impaired fertility and hypothyroidism secondary to endocrine disruption. Pentachlorophenol is a weak mutagen but the available data for humans are insufficient to classify it more strongly than as a probable carcinogen (Proudfoot 2003).

Pentachlorophenol may exhibit acetylcholinesterase (AChE) inhibitory activity (Igisu et al. 1993), however no research exists regarding the effects of its metabolites. Neuronal health is not dependent on cell viability alone, and many pesticides are known AChE inhibitors, thus assessment of effects on AChE was warranted to gain further insight into the potential of neurotransmitter activity disruption.

Various cell types appear to respond differently to PCP exposure, thus mechanisms of cell death in neurons cannot be assumed from investigations involving non-neuronal cells. Extrapolation of toxicity mechanisms from animal models is also limited due to different toxicokinetics between human and animal models. Effects on a human neuronal cell line would therefore provide greater insight into potential cytotoxic effects in human neurons. Shortfalls and gaps in current literature include a lack of studies on human neuronal cells, as well as a lack of consensus as to the mode of cell death induced by each of the compounds (Chen et al. 2014; Wang et al. 2000). Investigations involving only the parent compound or metabolite do not necessarily provide a complete picture, as metabolically altered compounds often exhibit vastly different action than the unaltered parent. Time-dependant studies are also required to identify a sequence of events leading to cell death, such that upstream events can be identified. In order to address these gaps, the aim of the study was therefore to evaluate the effects of PCP and its metabolites, TCBQ and TCHQ in human neuroblastoma SH-SY5Y cells.

2. Materials and Methods

2.1. Cell culture and treatments

SH-SY5Y human neuroblastoma cells (ATCC: CRL-2266) were cultured with a 1:1 ratio of Dulbecco's Modified Eagle's Medium (DMEM) and Ham’s F-12 nutrient mixture (Sigma-Aldrich, St. Louis, USA), containing 10% foetal calf serum (The Scientific Group, Gauteng, South Africa) at 37°C and 5% CO2. Cells were trypsinised approximately every two to three days by adding 1 mL TrypLE Express trypsin

(Thermo Fisher Scientific, Massachusetts, United States) after washing with phosphate buffered saline (PBS) (BD Bioscineces, Le Pont de Claix, France). Trypsin was neutralised with 1 mL medium, and detached cells were collected for either experimental purposes or further cell culture. For all experiments cells were seeded at a concentration of 50 000 cells/mL, and allowed a 24 h attachment period prior to compound or control exposure. All experiments made use of a relevant positive control, vehicle control (dimethyl sulfoxide; DMSO; Merck Millipore, Darmstadt, Germany), negative control (medium only), and colour control where appropriate. The concentration of DMSO in vehicle controls was equal to that of the highest DMSO concentration in test samples (< 0.5%).

2.2. Effect on cell proliferation

The sulforhodamine B (SRB) colorimetric assay was performed according to Vichai and Kirtikara (2006) to determine concentrations of each compound for which cell proliferation was inhibited by half (IC_{50}). Seeded cells were exposed to varying concentrations of PCP (Chem Service, West Chester, USA), TCBQ (Sigma-Aldrich, St. Louis, USA), TCHQ (Dr Ehrenstorfer, Augsburg, Germany), DDT (positive control) (Sigma-Aldrich, St. Louis, USA), or vehicle control. After 48 h incubation, 50% cold trichloroacetic acid (Merck Millipore, Darmstadt, Germany) was added to the wells and incubated at 4°C overnight for fixation. The plates were washed with tap water, and 0.057% SRB stain (Sigma-Aldrich, St. Louis, USA) added and incubated for 30 min. Excess dye was washed off with 1% acetic acid (Saarchem, Gauteng, South Africa), and 10 mM tris-base solution (Merck Millipore, Darmstadt, Germany) was added. Spectrophotometry was performed using a Biotek EL-X 800 microplate reader, with absorbance measured at 490 nm with a reference of 530 nm. Survival percent of test compounds compared to the vehicle control was determined, and IC_{50} values obtained from a non-linear regression curve (log[inhibitor] vs response function) generated using Graphpad Prism 6.

2.3. Cell cycle analysis

Cells were exposed to IC_{50} values of PCP, TCBQ, TCHQ, positive control (DDT), or vehicle control for 12, 24, and 48 h. Cells were then trypsinised, collected in separate 15 mL tubes, centrifuged at 300 *g* for 5 min, and the supernatant discarded. Cells were resuspended in cold PBS, and ice cold 70% ethanol. Cells were then centrifuged at 400 *g* for 10 min, and the supernatant discarded. A propidium iodide (PI)-RNase solution consisting of 100 µg/mL PI (Sigma-Aldrich, St. Louis, USA) and 40 ug/mL

RNase (Sigma-Aldrich, St. Louis, USA) in PBS was added. Samples were then incubated for 45 min at 37°C, and transferred to flow cytometry tubes. The DNA content of the cells was quantified using a Beckman Coulter FC500 series flow cytometer, under the FL3 channel. Data analysis was conducted using the Weasel flow cytometry analysis programme to determine average percent events in different cell cycle phases: sub-G1, G1, S, and G2/M phase for each time point. The same process was conducted to determine cell cycle effects of 48 h PCP exposure at varying concentrations.

2.4. Mode of cell death

Cells were exposed to test and control compounds and trypsinised as described in section 2.3. After 48 h exposure, samples were centrifuged, the supernatant discarded, and cells resuspended in binding buffer. The cells were again centrifuged, supernatant discarded, and cells resuspended in binding buffer, as well as Annexin V-FITC (Sigma-Aldrich, St. Louis, USA). Samples were incubated at 25°C in the dark for 15 min, followed by centrifuging at 300 *g* for 10 min. Cells were resuspended in binding buffer, and immediately prior to flow cytometry analysis, 30 µg/mL PI was added. Flow cytometry was performed using the Beckman Coulter FC500 series flow cytometer, and scatter plots produced, which were divided into four quadrants with different cell populations: Annexin V-FITC- /PI- events were determined as live cell populations, Annexin V-FITC+ /PI- as early apoptosis, Annexin V-FITC+ /PI+ as late apoptosis and Annexin V-FITC- /PI+ as necrosis. Gating was used to define quadrant boundaries according to the vehicle control of each run.

2.5. Caspase-3 activity

Cells were exposed to IC_{50} values of PCP, TCBQ, TCHQ (as determined in section 2.2), 20 µM) staurosporine (positive control) (Sigma-Aldrich, St. Louis, USA), or vehicle control for 48 h. Thirty minutes prior to starting the assay, 0.5 mM phenylmethylsulfonyl fluoride (PMSF) (Sigma-Aldrich, St. Louis, USA) and 4.3 mM β-mercaptoethanol (Merck Millipore, Darmstadt, Germany) were added to the incomplete lysis buffer, and 0.5 mM PMSF, 4.3 mM β-mercaptoethanol, and 5 µM AC-DEVD-AMC (Sigma-Aldrich, St. Louis, USA) were added to the incomplete caspase-3 substrate buffer. After the 48 h exposure period was complete, medium was replaced with cold lysis buffer and incubated on ice for 15 min. Caspase-3 substrate buffer was then added, and samples incubated at 37°C for 4 h. Thereafter, the plate was further incubated at 4°C for 16 h. The plate was then read using a BioTek Synergy 2 plate

reader, with excitation and emission wavelengths of 380 nm and 460 nm respectively. Fluorescence values were normalised according to cell density. Fold change of caspase-3 relative to vehicle control was obtained by dividing normalised test sample fluorescence by normalised vehicle control fluorescence.

2.6. Reactive oxygen species

Cells were exposed to IC_{50} values of PCP, TCBQ, TCHQ, 500 µM 2,2'-Azobis(2-amidinopropane) dihydrochloride (AAPH) (positive control) (Sigma-Aldrich, St. Louis, USA), or vehicle control for 4, 24, and 48 h. Cells were then trypsinised, collected in separate 15 mL tubes, centrifuged, and the supernatant discarded. Cells were resuspended in 10 µM 2,7-dichlorofluorescein diacetate (SigmaAldrich, St. Louis, USA) in PBS. Samples were incubated at 37°C for 15 min. Cells were then washed twice with PBS, after which cells were resuspended in PBS, and transferred to flow cytometry tubes. Green 2,7-dichlorofluorescein (DCF) fluorescence was quantified via flow cytometry for each sample using the Beckman Coulter FC500 series flow cytometer under an FL1 channel. Data obtained was analysed using Weasel flow cytometry software, and the mean fold change in ROS relative to DMSO was obtained for each time point.

2.7. Mitochondrial membrane potential

Cells were exposed to IC_{50} values of PCP, TCBQ, TCHQ, 100 nM rotenone (positive control) (SigmaAldrich, St. Louis, USA), or vehicle control for 4, 24, and 48 h. Cells were then trypsinised, collected in separate 15 mL tubes, centrifuged, the supernatant discarded, and cells resuspended in 5 µg/mL JC-1 dye (Sigma-Aldrich, St. Louis, USA) in PBS. After a 15 min incubation period at 37°C, cells were again centrifuged and washed twice with PBS. Thereafter, cells were resuspended in PBS and transferred to flow cytometry tubes. Fluorescence was measured using a Beckman Coulter FC500 series flow cytometer, under FL1 and FL2 channels. Mean fluorescence values were obtained from resulting histograms for both channels, the FL2/FL1 ratio of which was used to determine mitochondrial membrane potential ($\Delta\Psi m$) fold change relative to DMSO for each time point.

2.8. Glutathione content

Cells were exposed to IC_{50} values of PCP, TCBQ, TCHQ, 10 µM n-ethylmaleimide (NEM) (positive control) (Sigma-Aldrich, St. Louis, USA), or vehicle control for 48 h. Medium was then replaced with 16 µM monochlorobimane (Sigma-Aldrich, St. Louis, USA) in PBS and incubated at 37°C for 2 h. Fluorescence of each well was quantified spectrofluorometrically using a BioTek Synergy 2 plate reader with excitation and emission wavelengths of 360 nm and 460 nm respectively. Fluorescence values were normalised according to cell density, and glutathione (GSH) fold change relative to DMSO was obtained by dividing normalised test sample fluorescence by normalised vehicle control fluorescence.

2.9. Acetylcholinesterase inhibitory activity

The acellular Ellman esterase assay (Ellman et al. 1961) was used to determine effects on acetylcholinesterase (AChE) activity. Three buffers, namely A, B and C, were prepared prior to the start of the assay. Buffer A consisted of tris hydrochloride (Merck Millipore, Darmstadt, Germany) adjusted to pH 8, buffer B consisted of buffer A containing 0.1% bovine serum albumine (Sigma-Aldrich, St. Louis, USA), and buffer C consisted of buffer A containing 0.1 M sodium chloride and 0.02 M magnesium chloride hexahydrate (Merck Millipore, Darmstadt, Germany). Into a 96-well plate, 25 µL (15 mM) acetylthiocholine iodide (Sigma-Aldrich, St. Louis, USA) 125 µL (3 mM) 5,5′-dithiobis(2-nitrobenzoic acid) (Sigma-Aldrich, St. Louis, USA) (in buffer C), and 50 µL buffer B was added to each well. Cytotoxic IC_{50} concentrations of PCP, TCBQ, or TCHQ in buffer A were then added (initially, concentrations of compounds tested were the same as those used in cellular assays – here termed the 'cytotoxic IC_{50}). Water in buffer A served as a negative control, DMSO in buffer A as a vehicle control, and galanthamine (20 µM; Sigma-Aldrich, St Louis, USA) in buffer A as positive control. Baseline absorbance was measured in a plate reader at 405 nm at 45 s intervals for 3 intervals (read 1), in order to control for spontaneous acetylcholine (ACh) cleavage. Following this, 0.2 U/mL AChE (Sigma-Aldrich, St. Louis, USA) was added, and fluorescence measured again every 45 s, eight times consecutively (read 2). This initial rate kinetic run provided Vmax values for both reads, from which AChE activity was inferred. Percent AChE activity relative to DMSO was obtained from background adjusted Vmax values. The same assay was employed for a range of PCP, TCBQ and TCHQ concentrations. Ellman IC_{50} values (the concentration at which AChE activity is inhibited by half) were obtained from a non-linear regression curve (log[inhibitor] vs response function) using Graphpad Prism 6.

2.10. Statistical analysis

Spectrophotometry and spectrofluorometry based experiments were performed in at least triplicate, with a minimum of three biological repeats. Flow cytometry experiments were performed on at least three separate occasions, and a statistical power was ensured as each cell counted as an event, and a minimum of 10 000 events were obtained for each sample. Descriptive statistics were expressed as mean ± standard deviation. Data analysis was performed on Microsoft Excel 2010, Graphpad Prism 6 and Weasel flow cytometry software. Nonlinear regression was used to determine IC_{50} values. Significance of differences between two groups (vehicle control and test) was performed using a two tailed Student t-test. Alpha (α) was set at 0.05, and a p value below 0.05 was considered significant.

3. Results

3.1. Effect on cell proliferation

All three compounds exhibited cytotoxic effects in a dose-dependent manner, with IC_{50} values of 80.0±4.6, 35.4±1.6, and 63.7±3.1 µM for PCP, TCBQ, and TCHQ, respectively (Fig. 1). The lowest concentrations tested at which toxicity was induced were 70, 20, and 50 µM for PCP, TCBQ, and TCHQ, respectively. There were no significant differences between negative controls and vehicle (DMSO) controls throughout all experiments, unless otherwise stated.

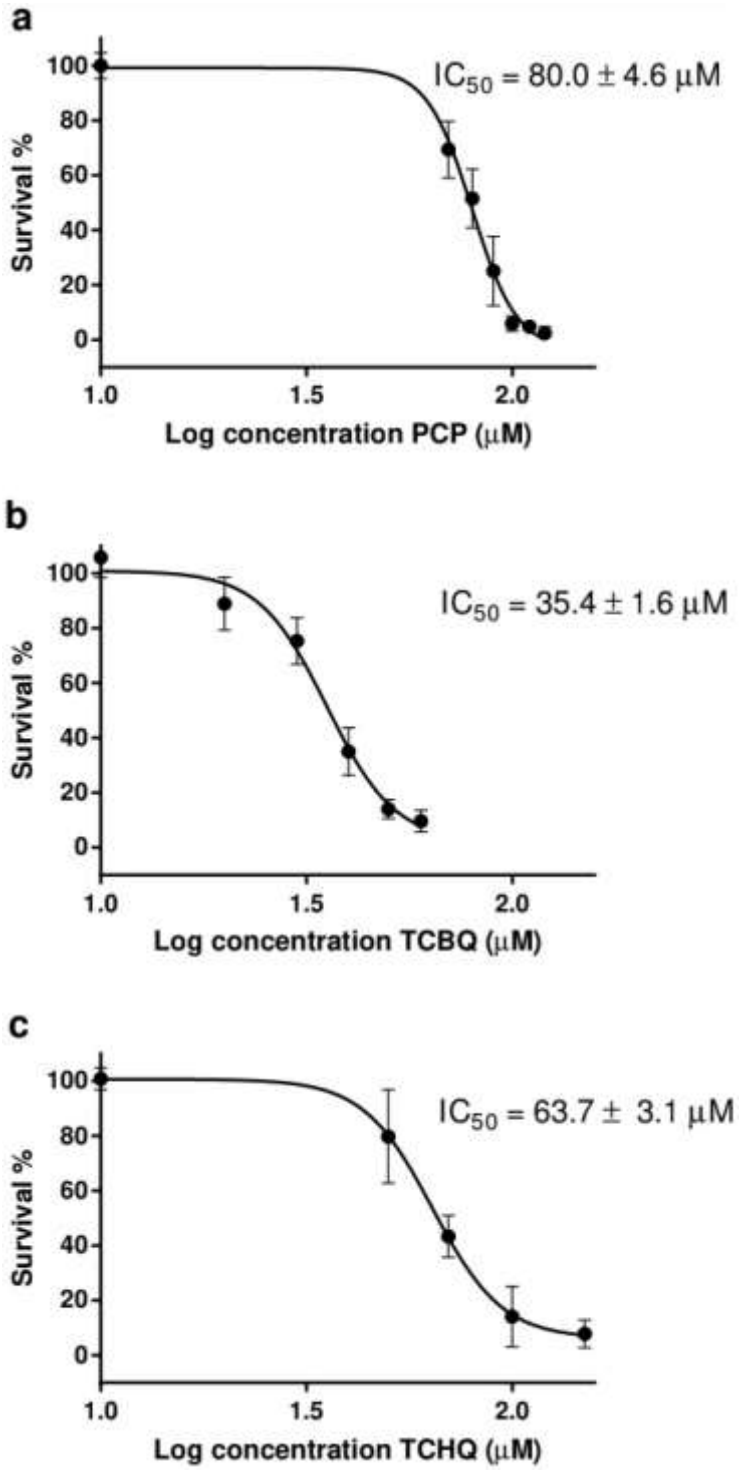

Fig. 1. Dose-response curves of cells treated with a) PCP, b) TCBQ, and c) TCHQ.

3.2. Cell cycle analysis

After 12 h exposure, 35 μM TCBQ caused an accumulation of cells in S phase, accompanied by a decrease in the G1 population, however no significant change occurred in the G2/M phase (Fig. 2a).

Sequential increases of events in the sub-G1 population were evident after 24 (Fig. 1b) and 48 h (Fig. 2c) exposure to TCBQ. The most pronounced effect was after 48 h incubation.

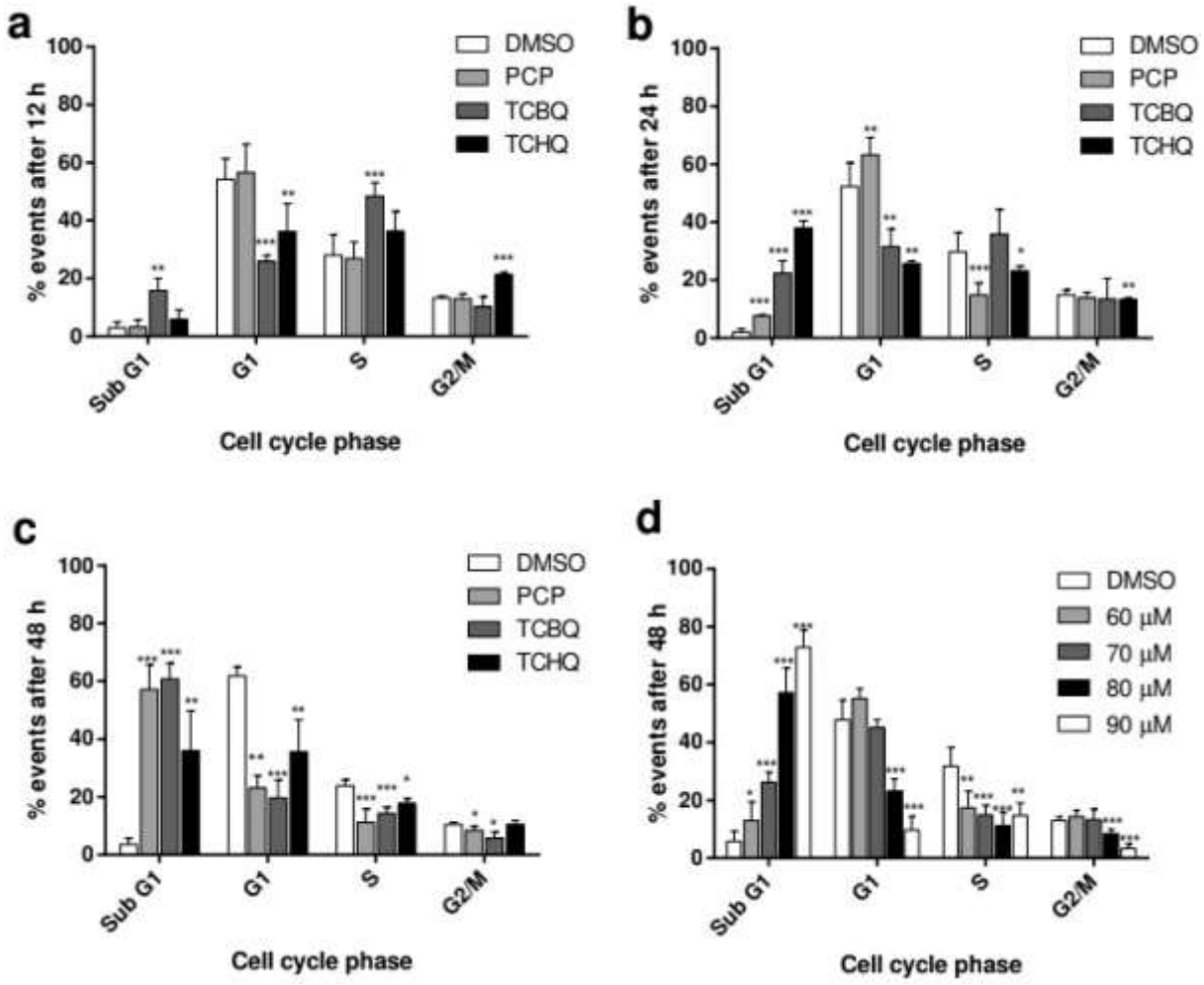

Fig. 2. Average percent events for each cell cycle phase after (a) 12 h, (b) 24 h, and (c) 48 h exposure to DMSO (vehicle control), PCP, TCBQ, or TCHQ. (d) Average percent events for each cell cycle phase after exposure to a range of PCP concentration. Significance of changes relative to vehicle control of the same cell cycle phase are indicated as $^{*}p < .05$, $^{**}p < .01$, $^{***}p < .001$.

After 12 h exposure to 63 µM TCHQ, an accumulation of cells in G2/M phase was observed, which was accompanied by a decrease of events in the G1 population (Fig. 2a). No increase in the sub-G1 phase was observed at this time point. After 24 h exposure however, there was an increase in the sub-G1 population, which was larger than the corresponding TCBQ sub-G1 population (Fig. 2b).

No change in cell cycle was observed following 12 h exposure to 80 µM PCP (Fig. 2a). After 24 h, PCP there was a significant ($p < 0.01$) increase in the number of events in the G1 phase (Fig. 2b). This was

accompanied by a decrease in the S phase, as well as an increase in the sub-G1 phase. After 48 h PCP exposure, the majority of events occurred in the sub-G1 fraction (Fig. 2c). Cell cycle analysis of a range of concentrations of PCP revealed a dose-dependent increase in the sub-G1 population (Fig. 2d).

3.3. Mode of cell death

All test exposure conditions resulted in significant ($p < 0.001$) decreases in live cell populations (Annexin V-FITC-/PI-) (Fig. 3a) after 48 h exposure. Exposure to PCP resulted in significant increases in Annexin V-FITC-/PI+ ($p < 0.01$) and Annexin V-FITC+/PI+ ($p < 0.05$) cells, and no significant increases in Annexin V-FITC+/PI-. Cells exposed to TCBQ displayed increases in Annexin V-FITC+/PI- and Annexin V-FITC+/PI+ cells, without any change in Annexin V-FITC-/PI+. Interestingly, cells exposed to TCHQ appeared to result in one of two fates. In the first instance (indicated as TCHQ 1 in Fig. 3a), there were increases in Annexin V-FITC+/PI- and Annexin V-FITC+/PI+ cells, with negligible change in the amount of Annexin V-FITC-/PI+ cells compared to the control. The second TCHQ-induced fate (indicated as TCHQ 2) resulted in significant ($p < 0.01$) increases in Annexin V-FITC+/PI+ and Annexin V-FITC-/PI+. The increase observed in Annexin V-FITC+/PI- cells was not significant when compared to DMSO. Thus, the first fate yielded cells predominantly expressing Annexin V-FITC, and the second fate predominantly expressing PI. The reduction in the number of live cells was greater in fate 2 than in fate 1. These results were concluded from 9 assay repeats, where 5 of the 9 repeats yielded fate 1, while 4 repeats yielded fate 2. Significant ($p < 0.001$) increases in caspase-3 activity were observed following 48 h exposure to all three compounds (Fig. 3b).

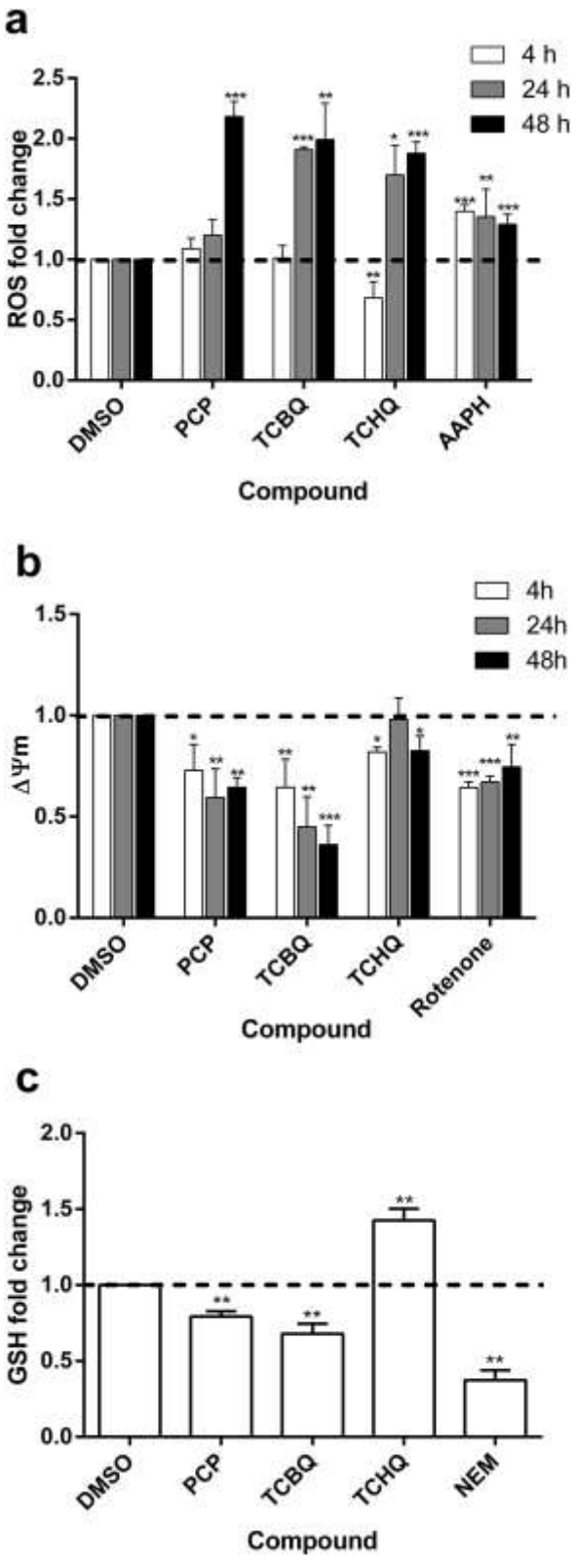

Fig. 3. (a) Mode of cell death following 48 h exposure to DMSO (vehicle control), PCP, TCBQ and TCHQ (1 and 2 indicate apoptotic and necrotic fates, respectively), and (b) Fold change in caspase-3 activity relative to DMSO following 48 h exposure to PCP, TCBQ, TCHQ or staurosporine (positive control). Significance is indicated by $^{\square}p < .05$, $^{\square\square}p < .01$, and $^{\square\square\square}p < .001$.

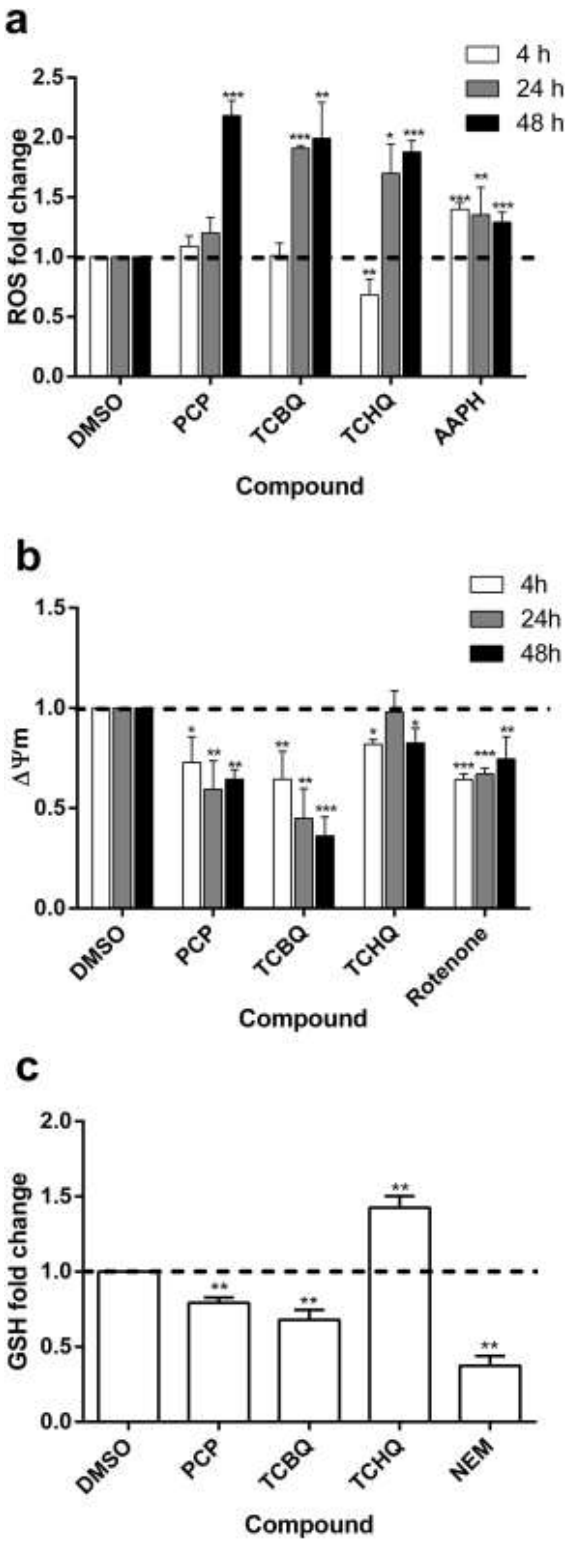

Fig. 4. Fold change in (a) reactive oxygen species (ROS) and (b) mitochondrial membrane potential (ΔΨM) relative to DMSO following 4, 24, or 48 h exposure to PCP, TCBQ, TCHQ, or positive control (ROS – AAPH; ΔΨM – rotenone). (c) Fold change in glutathione (GSH) relative to DMSO following 48 h exposure to PCP, TCBQ, TCHQ, or positive control (NEM). Significance of changes relative to vehicle control of the same cell cycle phase are indicated as $^{\square}p < .05$, $^{\square\square}p < .01$, $^{\square\square\square}p < .001$.

3.4. Reactive oxygen species, mitochondrial membrane potential, and glutathione

Exposure to PCP resulted in increased ROS after 48 h (Fig. 4a), while ΔΨm was reduced after 4 h (Fig. 4b). An increase in GSH was observed after 48 h. Exposure of cells to TCBQ resulted in similar effects on ROS, ΔΨm, and GSH (Figs. 4a-c) as noted for PCP, with the exception that ROS increased earlier, at 24 h as opposed to 48 h (Fig. 4a). An early event in TCHQ exposure was decreased ΔΨm after 4 h, which was recovered after 24 h, and again diminished after 48 h (Fig. 4b), while an increase in ROS was observed after 24 h (Fig. 4a). A significant ($p < 0.01$) increase in GSH was observed after 48 h TCHQ exposure (Fig. 4c).

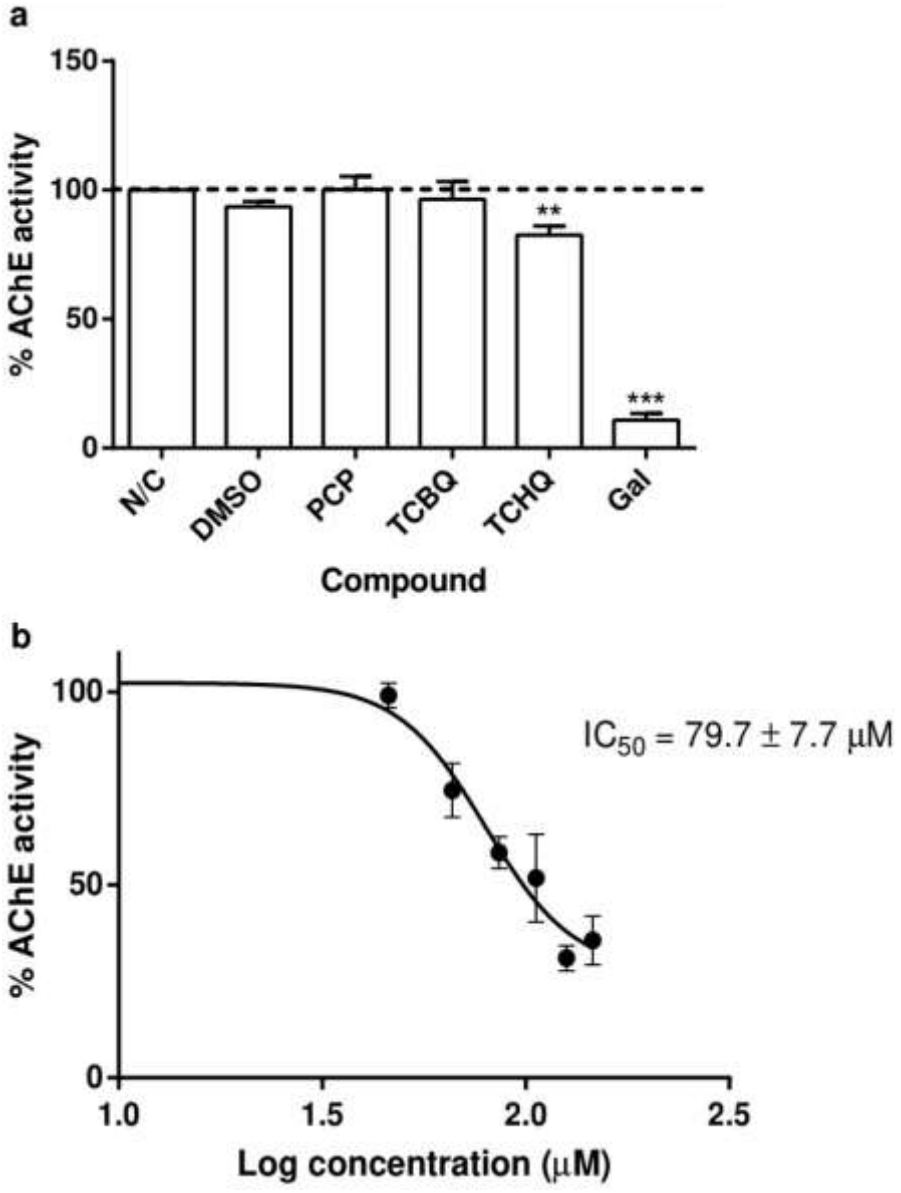

Fig. 5. (a) Effect of cytotoxic IC_{50} concentrations of PCP, TCBQ, and TCHQ, (concentrations determined from the SRB assay), on AChE activity. Significance is indicated by $^{\dagger}p < .01$ and $^{\square\square\square}p < .001$ when compared to DMSO (vehicle control). (b) Dose-response curve on the inhibitory activity of TCHQ on AChE.

3.5. Acetylcholinesterase inhibitory activity

A small, but significant ($p < 0.01$) decrease in AChE activity was observed between the negative and vehicle control. Cytotoxic cell growth IC_{50} concentrations (as determined by the SRB assay) of PCP and TCBQ had no effect on AChE activity compared to the vehicle control, while a small but significant ($p < 0.01$) decrease in activity occurred due to TCHQ (Fig. 5). Dose-response for TCHQ yielded an Ellman IC_{50} of 79.7±7.7 µM.

4. Discussion

4.1. Effect on cell proliferation

Steep dose-response curves indicated a narrow range between the IC_{50} values and the lowest concentrations at which toxicity is induced. Concentrations at which the compounds induced cytotoxic action were fairly high micromolar ranges, indicating that acute toxicity symptoms would be unlikely in people without occupational exposure, or in areas devoid of environmental contamination. Given the bioaccumulation characteristic of PCP (bioconcentration factor of 3.3 in the brain (Geyer et al. 1987)), toxic effects may be more probable in conditions of chronic exposure than acute exposure. High effective concentrations may pose a paradoxical risk scenario, wherein the occurrence of toxicity may be classified as low, however gradual alterations to neuronal cell functioning after chronic exposure may not allow for adequate detection thereof. Investigation into thresholds at which PCP and its metabolites induce notable symptoms *in vivo* would be beneficial to fully quantify the risk. While no previous studies have assessed the toxicity of both PCP and its metabolites in SH-SY5Y cells, the dose-dependent effects are in accordance with toxicity found in other mammalian neuronal cell lines (Folch et al. 2009; Fu et al. 2017; Tanaka et al. 2005).

4.2. Cell cycle analysis

The distribution of cell populations after 12 h TCBQ exposure suggests a prolonged traverse of cells through S phase, which ultimately fall out of cell cycling before the G1 phase is reached. Delay or failure of cells passage to G2 phase likely contributed to a cascade of events leading to apoptosis (Cuddihy and O'Connell 2003), which is already seen after 12 h by an increased sub-G1 population. Sequential increases of events in the sub-G1 population suggest that while apoptosis may occur as early as 12 h after exposure, the bulk of apoptosis occurs after more extended TCBQ exposure.

A classic G2/M phase block was evident following 12 h TCHQ exposure. This was likely due to the activation and maintenance of the G2/M checkpoint (Lobrich and Jeggo 2007). Cells remaining at the G2/M boundary for extended periods are reported to subsequently undergo cell death (DiPaola 2002). A more rapid onset of cell death by TCBQ than TCHQ was evident after at least a 12 h delay.

After 24 h, PCP exerted a G1 block and increased the sub-G1 population, indicating cell cycle exit before entry into the S phase. Considering the ability of PCP to uncouple oxidative phosphorylation, and the elevated ROS production observed in the present study (section 4.4), it is possible that oxidative stress stimuli contributed to the G1 arrest. After 48 h PCP exposure, the evidence of a G1 block had subsided. Cell cycle analysis of a range of concentrations of PCP revealed a dose-dependent increase in the sub-G1 population, which supports the dose-dependent effect on cell growth observed in the SRB assay. This is corroborated by Yang et al. (2005), who also found time- and dose-dependent cell death as a result of PCP exposure in rat Sertoli cells. The timing of PCP cell cycle disruptions compared to the metabolites indicated that the two metabolites act more quickly than the parent compound. Surprisingly few studies have evaluated the effect of PCP and its metabolites on cell cycle, however some studies have made use of cell cycle analysis to assess DNA fragmentation denoted by the sub-G1 population. DNA fragmentation is most frequently associated with apoptosis, however, is known to occur in necrotic cell death as well. This is particularly so for ROS-mediated necrosis, where oxidative damage incurs DNA strand breaks (Higuchi 2003). Apoptotic or necrotic DNA fragmentation, or a combination thereof has been described for PCP, and may be cell type dependent (Chen et al. 2004).

4.3. Mode of cell death

Annexin V-FITC/PI fluorescence characteristics as well as caspase-3 activity was used to determine the predominant mode of cell death for each compound. The accompaniment of increased caspase-3 activity with predominantly Annexin V-FITC- /PI+ fluorescence indicated that both apoptotic and necrotic mechanisms were present following PCP exposure. It is possible that apoptosis was initiated, and subsequently converted to necrosis upon the early occurrence of mitochondrial disruptions. Apoptosis is an energy dependent processes, thus disruption of cellular metabolism due to $\Delta\Psi m$ collapse may leave the cell depart of sufficient ATP to carry apoptosis through to completion. Consensus has not been reached in literature with regards to the mode of cell death for PCP, which may be dependent on the

tolerance of different cell types to metabolic and redox disruption (Heusinkveld and Westerink 2017). Neuronal cells are often more sensitive to metabolic disruption, and therefore may be more susceptible to a necrotic pathway following PCP exposure. Necrotic mechanisms were not apparent for TCBQ, which displayed more classical apoptosis characteristics. Unlike PCP, this is agreed on in literature.

Exposure of cells to TCHQ presented with an interesting case, as it appeared to induce either predominantly apoptotic (fate 1) or necrotic like cell death (fate 2) in different biological samples. It was noted that fate 1 appeared to be the less potent outcome. Similar to PCP, apoptosis may have been initiated, and converted to necrosis in fate 2, while apoptosis was initiated and followed through to completion in TCHQ fate 1. Cell cycle was not synchronised, which may have contributed to the difference in fates. Fate 2 may have occurred in cells starting closer to the G2/M phase, as the longer cells remain blockaded at this phase, the more susceptible they are to undergo necrosis than other cell cycle blocks (DiPaola 2002). The timing of cell cycle disruptions observed coincided with the timing of ΔΨm and redox events described in section 4.4, thus the mechanisms of cell death appear to be linked to cell cycle. The presence of Annexin V-FITC- /PI+ cells in fate 2 indicated that PI fluorescence was not the result of advanced apoptosis, but definite occurrence of primary necrosis. The propensity for cells to differentially undergo apoptosis or necrosis as a result of TCHQ exposure has been previously described in splenocytes, which ascribed the phenomenon to ROS effects (Chen et al. 2014).

4.4. Reactive oxygen species, mitochondrial membrane potential, and glutathione

The timing of ROS and ΔΨm disturbances indicate that effects occurred first in the mitochondria. This timing suggests that an initial cause of ROS increase was due to the leakage of electrons from a compromised mitochondrial membrane, which subsequently formed ROS. Although the initiation of ROS-ΔΨm events occurred in the mitochondria, the resultant increased production of ROS would create a vicious cycle of further ΔΨm reduction and ROS production (Zorov et al. 2014). Pentachlorophenol is known to uncouple oxidative phosphorylation, a process which may recruit uncoupling proteins (Jastroch et al. 2010). This process may allow for inappropriate passage of protons to the mitochondrial matrix, thus impairing ATP production, as well as electron leakage through a permeabilized mitochondrial membrane (Kadenbach 2003), which may have contributed to the observed reduction in ΔΨm. Fernandez Freire et al. (2005) attributed lysosome destabilisation to PCP-induced disruption of

mitochondrial function, which may explain the observed necrotic cell death, as this mechanism is commonly associated with necrosis (Guicciardi and Gores 2013). The uncoupling of oxidative phosphorylation and mitochondrial dysfunction arising from PCP exposure may result in an impaired ability for ATP production, favouring necrosis to apoptosis. The role of mitochondrial disruption and ROS in cytotoxic effects of PCP has been described in a number of instances (Chen et al. 2015; Dong et al. 2009; Folch et al. 2009; Jiang et al. 2016), and is confirmed for SH-SY5Y cells in the present study. Furthermore, this study demonstrates that ΔΨM disruption occurs prior to ROS increase. Depletion of GSH was observed following 48 h PCP exposure (Fig. 4c), and was likely reduced by excessive ROS, leaving cells vulnerable to oxidative stress. Decreased GSH has been reported due to PCP exposure in hepatocytes (Dong et al. 2009; Jiang et al. 2016), however the effect of PCP on GSH levels has not previously been directly examined in neuronal cells.

The quicker increase in ROS following TCBQ exposure compared to PCP indicated faster acting ROS production mechanisms. The quicker increase in ROS for TCBQ (and TCHQ) exposed cells may be linked to cell cycle, as effects on cell cycle also appeared earlier for metabolite exposure, and coincided with these events. Appropriate cell cycle progression is reliant on appropriate ROS and GSH levels, and alterations thereof may exacerbate cell cycle disruption and toxicity in cells sensitive to ROS fluctuation (Boonstra and Post 2004; Diaz Vivancos et al. 2010; Heusinkveld and Westerink 2017).

The transient ΔΨm recovery observed following TCHQ exposure may have contributed to ultimate cell fate. If mitochondrial functioning is recovered for long enough, sufficient ATP may be produced to see apoptosis through to completion, while a shorter recovery period may eventuate necrosis due to insufficient ATP production. Recovery of ΔΨm has been reported to protect cells against necrosis (Sunaga et al. 2014), however this particular concept has not been previously explored in TCHQ toxicity, as no time-dependent studies have been conducted. Endpoint ΔΨm decreases have however been reported for TCHQ in different cell lines, and similar to the present study, has also been linked to increased ROS production (Chen et al. 2015; Jiang et al. 2016). An unexpected result of TCHQ was the increase in GSH. Increased GSH is usually associated with increased cell proliferation (Traverso et al. 2013), however its role in toxicity has been described in the form of reductive stress (Zhang et al. 2012). Less common than oxidative stress, this process has the potential to exert pathological effects by

inappropriately reducing cellular components due to the altered redox status of elevated GSH levels (Lemasters and Nieminen 1997). Although increased GSH would confer enhanced antioxidant activity against ROS, a paradoxical effect of further increased ROS production in an environment of reductive stress has been recently described (Korge et al. 2015). This ROS increase, accompanied by ROS derived from other processes such as mitochondrial damage, results in a net increase in ROS despite greater antioxidant activity, thereby switching toxic actions from reductive to oxidative stress (Pervaiz and Clement 2002).

4.5. Acetylcholinesterase inhibitory activity

The decrease in AChE activity between the negative and vehicle control was to be expected as DMSO is known to inhibit AChE activity (Kumar and Darreh-Shori 2017). The Ellman IC_{50} was higher than the corresponding cytotoxic IC_{50}. This suggests that cytotoxic effects would occur at lower concentrations before neurotransmitter irregularities would arise, however this would require further validation *in vivo*. Although the Ellman IC_{50} was higher, it was not vastly departed from the corresponding cytotoxic IC_{50}, thus at chronic concentrations, cytotoxic and neurotransmitter effects may quickly overlap and compound one another to produce greater overall toxicity (Colovic et al. 2013). No previous studies have explored TCHQ inhibition of AChE, however other pesticides such as carbamates and organophosphates are known to inhibit AChE. Pentachorophenol has been reported to inhibit AChE activity only at very high concentrations (approximately 750 µM) (Igisu et al. 1993). This data provides insight into the role of neurotransmitter disruption in the toxicity of these compounds towards neuronal cells, however further investigation is required to clarify its contribution and interactions thereof.

Limitations of the study were that only single concentrations of the test compounds were used in most of the parameters examined.

5. Conclusions

The three compounds exhibited different mechanisms of toxicity leading to different modes of cell death in neuronal cells. Two fates existed for cells exposed to TCHQ, apoptosis or necrosis, which may have been linked to transient ΔΨM recovery and redox stress. Early mitochondrial disruptions and oxidative stress ultimately contributed to necrosis in PCP exposed cells, while the completion of apoptosis was

avoided. TCBQ exhibited classic apoptotic effects. Reduced ΔΨM was found to precede redox disruptions for all compounds, indicating mitochondrial dysfunction to be an upstream event in cell death. Events leading to cell death appeared to coincided with cell cycle disruptions, which were also different for each compound. Further to cytotoxicity, AChE inhibition was noted for TCHQ only. To the authors' knowledge, this is the first study to evaluate the effects of TCBQ and TCHQ on AChE inhibitory activity. The present study is one of the few investigations comparing the toxic effects of PCP in conjunction with TCBQ, and THCQ in human neuronal cells at different time points, and provides insight into the sequence of events preceding cell death. The different modes of toxicity noted highlight the importance of assessing the parent compound in conjunction with the metabolites, as one cannot be extrapolated from the other.

Acknowledgement Funding was received from the National Research Foundation and Research Committee of the School of Medicine, University of Pretoria to carry out this project.

Conflict of Interest The authors declare that they have no conflict of interest.

References

Ateeq B, Abul Farah M, Niamat Ali M, Ahmad W (2002) Clastogenicity of pentachlorophenol, 2,4-D and butachlor evaluated by Allium root tip test Mutat Res 514(1-2):105-113

ATSDR (2001) Toxicological profile for Pentachlorophenol. Update. Atlanta, GA: U.S. Department of Health and Human Services, Public Health Service.

Boonstra J, Post JA (2004) Molecular events associated with reactive oxygen species and cell cycle progression in mammalian cells Gene 337:1-13

Chen HM, Lee YH, Wang YJ (2015) ROS-triggered signaling pathways involved in the cytotoxicity and tumor promotion effects of pentachlorophenol and tetrachlorohydroquinone Chem Res Toxicol 28(3):339-350

Chen HM, Zhu BZ, Chen RJ, Wang BJ, Wang YJ (2014) The pentachlorophenol metabolite tetrachlorohydroquinone induces massive ROS and prolonged p-ERK expression in splenocytes, leading to inhibition of apoptosis and necrotic cell death PLoS One 9(2):e89483

Chen J, Jiang J, Zhang F, Yu H, Zhang J (2004) Cytotoxic effects of environmentally relevant chlorophenols on L929 cells and their mechanisms Cell Biol Toxicol 20(3):183-196

Colovic MB, Krstic DZ, Lazarevic-Pasti TD, Bondzic AM, Vasic VM (2013) Acetylcholinesterase inhibitors: pharmacology and toxicology Curr Neuropharmacol 11(3):315-335

Cuddihy AR, O'Connell MJ (2003) Cell-cycle responses to DNA damage in G2 Int Rev Cytol 222:99-140

Diaz Vivancos P, Wolff T, Markovic J, Pallardo FV, Foyer CH (2010) A nuclear glutathione cycle within the cell cycle Biochem J 431(2):169-178

DiPaola RS (2002) To arrest or not to g-m cell-cycle arrest Clin Cancer Res 8(11):3311

Dong YL, Zhou PJ, Jiang SY, Pan XW, Zhao XH (2009) Induction of oxidative stress and apoptosis by pentachlorophenol in primary cultures of Carassius carassius hepatocytes Comp Biochem Physiol C Toxicol Pharmacol 150(2):179-185

Ellman GL, Courtney KD, Andres V, Jr., Feather-Stone RM (1961) A new and rapid colorimetric determination of acetylcholinesterase activity Biochem Pharmacol 7:88-95

Fernandez Freire P, Labrador V, Perez Martin JM, Hazen MJ (2005) Cytotoxic effects in mammalian Vero cells exposed to pentachlorophenol Toxicology 210(1):37-44
Folch J, Yeste-Velasco M, Alvira D, de la Torre AV, Bordas M, Lopez M, Sureda FX, Rimbau V, Camins A, Pallas M (2009) Evaluation of pathways involved in pentachlorophenol-induced apoptosis in rat neurons Neurotoxicology 30(3):451-458
Fu J, Shi Q, Song X, Xia X, Su C, Liu Z, Song E, Song Y (2016) Tetrachlorobenzoquinone exhibits neurotoxicity by inducing inflammatory responses through ROS-mediated IKK/IkappaB/NF-kappaB signaling Environ Toxicol Pharmacol 41:241-250
Fu J, Xia X, Liu Z, Wang Y, Wang Y, Shi Q, Song X, Song E, Song Y (2017) The acute exposure of tetrachloro-p-benzoquinone (a.k.a. chloranil) triggers inflammation and neurological dysfunction via Toll-like receptor 4 signaling: The protective role of melatonin preconditioning Toxicology 381:39-50
Geyer HJ, Scheunert I, Korte F (1987) Distribution and bioconcentration potential of the environmental chemical pentachlorophenol (PCP) in different tissues of humans Chemosphere 16(4):887-899
Guicciardi ME, Gores GJ (2013) Complete lysosomal disruption: a route to necrosis, not to the inflammasome Cell Cycle 12(13):1995
Guo Y, Zhou B (2013) Thyroid endocrine system disruption by pentachlorophenol: an *in vitro* and *in vivo* assay Aquat Toxicol 142-143:138-145
Heusinkveld HJ, Westerink RHS (2017) Comparison of different in vitro cell models for the assessment of pesticide-induced dopaminergic neurotoxicity Toxicol In Vitro 45(Pt 1):81-88
Higuchi Y (2003) Chromosomal DNA fragmentation in apoptosis and necrosis induced by oxidative stress Biochem Pharmacol 66(8):1527-1535
Igisu H, Hamasaki N, Ikeda M (1993) Highly cooperative inhibition of acetylcholinesterase by pentachlorophenol in human erythrocytes Biochem Pharmacol 46(1):175-177
Jastroch M, Divakaruni AS, Mookerjee S, Treberg JR, Brand MD (2010) Mitochondrial proton and electron leaks Essays Biochem 47:53-67
Jiang P, Wang J, Zhang J, Dai J (2016) Effects of pentachlorophenol on the detoxification system in white-rumped munia (*Lonchura striata*) J Environ Sci (China) 44:224-234
Jones KC, de Voogt P (1999) Persistent organic pollutants (POPs): state of the science Environ Pollut 100(1-3):209-221
Juhl U, Witte I, Butte W (1985) Metabolism of pentachlorophenol to tetrachlorohydroquinone by human liver homogenate Bull Environ Contam Toxicol 35(5):596-601
Kadenbach B (2003) Intrinsic and extrinsic uncoupling of oxidative phosphorylation Biochim Biophys Acta 1604(2):77-94
Korge P, Calmettes G, Weiss JN (2015) Increased reactive oxygen species production during reductive stress: The roles of mitochondrial glutathione and thioredoxin reductases Biochim Biophys Acta 1847(6-7):514-525
Kumar A, Darreh-Shori T (2017) DMSO: A mixed-competitive inhibitor of human acetylcholinesterase ACS Chem Neurosci 8(12):2618-2625
Lemasters JJ, Nieminen AL (1997) Mitochondrial oxygen radical formation during reductive and oxidative stress to intact hepatocytes Biosci Rep 17(3):281-291
Li C, Wang F, Wang H (2017) Tetrachloro-1,4-benzoquinone induces apoptosis of mouse embryonic stem cells J Environ Sci (China) 51:5-12
Lobrich M, Jeggo PA (2007) The impact of a negligent G2/M checkpoint on genomic instability and cancer induction Nat Rev Cancer 7(11):861-869
Pervaiz S, Clement MV (2002) Hydrogen peroxide-induced apoptosis: oxidative or reductive stress? Methods Enzymol 352:150-159
Proudfoot AT (2003) Pentachlorophenol poisoning Toxicol Rev 22(1):3-11
Schroeder I (2011) MSc dissertation: A mechanistic study of organochlorine hepatotoxicity. dissertation, University of Pretoria
Sunaga D, Tanno M, Kuno A, Ishikawa S, Ogasawara M, Yano T, Miki T, Miura T (2014) Accelerated recovery of mitochondrial membrane potential by GSK-3beta inactivation affords cardiomyocytes protection from oxidant-induced necrosis PLoS One 9(11):e112529
Tanaka M, Ishizaka Y, Tosuji H, Kunimoto M, Hosoya N, Nishihara N, Kadono T, Kawano T, Kosaka T, Hosoya H (2005) A new bioassay for toxic chemicals using green Paramecia, *Paramecium bursaria*. In: Lichtfouse E, Schwarzbauer J, Robert D (eds) Environmental Chemistry: Green Chemistry and Pollutants in Ecosystems. Springer Science & Business Media, Berlin, p 676
Traverso N, Ricciarelli R, Nitti M, Marengo B, Furfaro AL, Pronzato MA, Marinari UM, Domenicotti C (2013) Role of glutathione in cancer progression and chemoresistance Oxid Med Cell Longev 2013:972913

Vichai V, Kirtikara K (2006) Sulforhodamine B colorimetric assay for cytotoxicity screening Nat Protoc 1(3):1112-1116
Wang YJ, Ho YS, Chu SW, Lien HJ, Liu TH, Lin JK (1997) Induction of glutathione depletion, p53 protein accumulation and cellular transformation by tetrachlorohydroquinone, a toxic metabolite of pentachlorophenol Chem Biol Interact 105(1):1-16
Wang YJ, Ho YS, Jeng JH, Su HJ, Lee CC (2000) Different cell death mechanisms and gene expression in human cells induced by pentachlorophenol and its major metabolite, tetrachlorohydroquinone Chem Biol Interact 128(3):173-188
Wang YJ, Lin JK (1995) Estimation of selected phenols in drinking water with in situ acetylation and study on the DNA damaging properties of polychlorinated phenols Arch Environ Contam Toxicol 28(4):537-542
Xu T, Yin J, Chen S, Zhang D, Wang H (2018) Elevated 8-oxo-7,8-dihydro-2'-deoxyguanosine in genome of T24 bladder cancer cells induced by halobenzoquinones J Environ Sci (China) 63:133-139
Yang S, Han X, Wei C, Chen J, Yin D (2005) The toxic effects of pentachlorophenol on rat Sertoli cells *in vitro* Environ Toxicol Pharmacol 20(1):182-187
Zhang H, Limphong P, Pieper J, Liu Q, Rodesch CK, Christians E, Benjamin IJ (2012) Glutathione-dependent reductive stress triggers mitochondrial oxidation and cytotoxicity FASEB J 26(4):1442-1451
Zhao B, Yang Y, Wang X, Chong Z, Yin R, Song SH, Zhao C, Li C, Huang H, Sun BF, Wu D, Jin KX, Song M, Zhu BZ, Jiang G, Rendtlew Danielsen JM, Xu GL, Yang YG, Wang H (2014) Redox-active quinones induces genome-wide DNA methylation changes by an iron-mediated and Tet-dependent mechanism Nucleic Acids Res 42(3):1593-1605
Zorov DB, Juhaszova M, Sollott SJ (2014) Mitochondrial reactive oxygen species (ROS) and ROS-induced ROS release Physiol Rev 94(3):909-950